5 Food rheology

C.D. RIELLY

Introduction

Fluids such as air and water have simple flow properties which are not functions of the previous process history of the material. Food materials are more complex, however, and their flow properties may be strong functions of the way in which they have been previously processed. For example, the flow behaviour of a yoghurt is a function of the bonding between the molecular chains of the protein aggregates which constitute it; if those bonds are disrupted by stirring or pumping, the flow properties of the material may change. This can be seen clearly by comparing a set and stirred yogurt bought from a supermarket and containing the same ingredients; the set material behaves essentially as a solid, whilst the stirred yoghurt has properties more like a liquid.

This chapter outlines approaches to the study of food rheology, the science of flow and deformation of materials. The simple fluids described up to now have had viscosities which are not functions of the fluid conditions: these are called Newtonian fluids. A series of models exist to describe more complicated, non-Newtonian, fluid systems, where the apparent viscosity changes with the process history and current conditions of the system. If the flow properties of a fluid can be described satisfactorily by such a model, then it is possible to carry out the sort of calculations introduced in Chapter 2, i.e. to predict flow rates, pressure drops and velocity distributions within systems.

Foodstuffs may exhibit non-Newtonian behaviour because they contain long-chain molecules, or solid particles, whose interactions depend on the rate at which the material is deformed. In some cases, the textures of water-based food products may be enhanced by addition of a polymer thickener: for example, addition of carboxymethyl cellulose (cmc) solutions to fruit drinks, or addition of xanthan gum to sauces or soups. These additives make the product appear 'thicker', something which in the mind of the consumer may be allied to higher concentration or better quality. However, they can also cause unacceptable changes to the foodstuff: the presence of 'wobbliness' caused by a large amount of elasticity, or 'stringiness' caused

Chemical Engineering for the Food Industry. Edited by P.J. Fryer, D.L. Pyle and C.D. Rielly. Published in 1997 by Blackie A & P, an imprint of Chapman & Hall, London. ISBN 0 412 49500 7

by having a large extensional viscosity (see section 5.1.5) may detract from the visual appearance of the product and its mouthfeel. The choice of these additives, from a rheological point of view, is critical to the formulation of textured foodstuffs, and one scientific method of determining the effect of various food additives on the perceived quality of food materials is to measure their flow behaviour in well-defined viscometric tests. In this chapter we shall discuss various concepts of non-Newtonian rheology and the engineering methods available to characterize the flow behaviour of complex food materials. Finally, we shall demonstrate how the various non-Newtonian constitutive equations can be incorporated into the solution of some engineering problems in the food processing industries.

Characterization

Many food materials have distinct physical properties in addition to their nutritional value, and it is often these rheological characteristics that make a significant contribution to the overall quality of the product. For example, to the consumer, the flow characteristics of tomato sauce pouring from a bottle may be as important as the taste; similarly the mouthfeel of a yoghurt (determined by its rheological properties) probably contributes as much to the pleasure of eating as does the flavour! It is therefore essential to be able to characterize the physical characteristics of the food in an exact and scientific way. Rheological testing may be carried out to ensure intermediate or final product quality control during prolonged batch or continuous operation (using in-line viscometers, which are accurate and can measure some non-Newtonian features of the fluid). It is also important to be able to correlate measured rheological parameters against consumer preference, allowing suitable choice of viscosity enhancers and giving a better understanding of ingredient functionality for new products. In the longer term it may be possible to correlate rheological characteristics against organoleptic properties determined by a taste panel, thereby producing a continuous and reproducible measurement of food texture.

Engineering processes

The rheological properties obtained from viscometric tests may be represented in terms of a constitutive equation (an equation relating material properties) describing the relationship between the rate of strain in the fluid and the applied shear stress. Solution of the momentum equations (see Chapter 2 for a discussion of Newtonian fluid mechanics) for fluid flow requires a knowledge of such a constitutive relation and allows prediction of the fluid flow behaviour in a number of engineering applications. Once foods have been rheologically characterized, then the same fluid mechanics approaches may (in principle) be used for non-Newtonian fluids, but using

a different form of the constitutive equation relating the shear stress to the strain rate. In some cases it may be possible to treat the fluid as a Newtonian liquid, but in others this assumption could give seriously misleading predictions. We shall discuss the various forms of non-Newtonian behaviour and show which constitutive equations are best suited to model various rheological characteristics. Worked examples are used to illustrate use of these methods in realistic engineering problems: for example, calculation of the pressure drop for flow of a non-Newtonian fluid through a long pipeline.

Shear forces and viscosity

A fluid in motion can sustain both shear and normal stresses, which are determined by the rate of strain and physical properties of the fluid. A normal stress is one that acts perpendicular to a hypothetical plane (pressure is an example of an isotropic normal stress), whereas a shear stress acts tangentially to a plane. In this chapter we are mainly concerned with shear stresses. An example of a simple shear flow is shown in Fig. 5.1: fluid is sheared between a fixed lower plate and an upper plate moving at a velocity v.

For this situation, **Newton's law of fluid friction** relates the shear stress in the fluid, τ_{yx}, to the velocity gradient, dv_x/dy:

$$\tau_{yx} = \mu \dot{\gamma}_{yx} = \mu \frac{dv_x}{dy} = \mu \frac{v}{a} \tag{5.1}$$

where μ is a coefficient of viscosity, and $\dot{\gamma}_{yx}$ is the rate of strain (alternatively called the shear rate). In this simple case the rate of strain is equal to the velocity gradient dv_x/dy, and the shear stress acting in the fluid is constant. However, in general τ_{yx} depends on the distance y from the wall: for example, in pipe flow (see section 2.3.2), the shear stress increases linearly from zero on the pipe centreline to the wall shear stress value.

The SI units for viscosity are Pa s, or alternatively $N\,s\,m^{-2}$, the shear stress is given in Pa or $N\,m^{-2}$ and the shear rate is in s^{-1}. Many older texts use

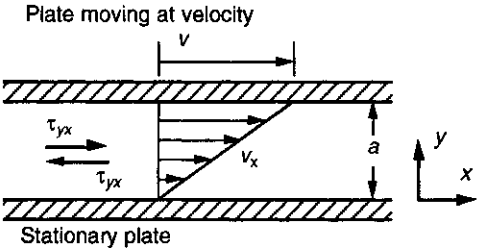

Fig. 5.1 Simple shear flow between two flat plates.

centipoise (cP) as the unit of viscosity, which is often convenient as water has a coefficient of viscosity at 25 °C of almost exactly 1 cP. To convert to SI units (which are used throughout this book) we use 1 cP = 0.001 Pa s. For Newtonian fluids the symbol μ represents the absolute viscosity; a kinematic viscosity, $\nu = \mu/\rho$ is also sometimes used in fluid mechanics and has units of $m^2 s^{-1}$.

Steffe (1992) gives some examples of the wide range of viscosities covered by Newtonian food fluids: water, 0.001 Pa s; coffee cream, 0.01 Pa s; vegetable oil, 0.1 Pa s; and honey 10 Pa s.

In more complicated three-dimensional flows there are six shear stresses and three normal stresses acting within the fluid. Figure 5.2 shows the stresses acting on three orthogonal faces of an element of fluid in Cartesian coordinates. The stresses σ_{xx}, σ_{yy} and σ_{zz} are known as the normal stresses, and for a Newtonian fluid in shear flow are equal to the isotropic pressure within the fluid, such that

$$\sigma_{xx} - \sigma_{yy} = 0$$

and

$$\sigma_{yy} - \sigma_{zz} = 0 \tag{5.2}$$

The shear stresses acting on the plane in the z direction (shown shaded) are τ_{zx} and τ_{zy}.

Thus for the simple shear flow of Fig. 5.1, $\tau_{yx} = \mu\dot{\gamma}_{yx}$ and $\tau_{xz} = \tau_{yz} = 0$. Note that the first subscript indicates the direction of the plane in which the shear stress lies and the second gives the direction in which it acts. By considering the moments of the forces due to shearing stresses it is also easy to show that

$$\tau_{xy} = \tau_{yx}, \qquad \tau_{xz} = \tau_{zx} \qquad \text{and} \qquad \tau_{yz} = \tau_{zy} \tag{5.3}$$

so that there are really only six independent stresses within the fluid. For most of the flows considered in this chapter it will be sufficient to work

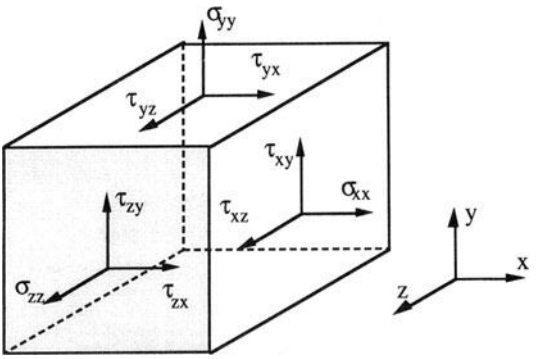

Fig. 5.2 Shear stresses and normal stresses acting in a fluid.

with one-dimensional fluid motion, and in this case we shall simply represent the appropriate shear stress by τ and the shear rate by $\dot{\gamma}$. The reader is referred to Barnes *et al.* (1989), Tanner (1985) or Tritton (1988) for more detailed discussions of three-dimensional rheology and fluid mechanics.

For Newtonian fluids the viscosity in equation (5.1) is a constant material property. However, the fluids that we shall consider in the remainder of this chapter have some internal structure, such that the viscosity depends on the rate at which the fluid is sheared; the viscosity may also depend on the time or history of the flow deformation. These are called non-Newtonian fluids, and in the next section we shall examine how the **apparent viscosity**, $\mu_a(\dot{\gamma})$, defined by

$$\mu_a(\dot{\gamma}) = \frac{\tau}{\dot{\gamma}} \tag{5.4}$$

changes with time and shear rate. In the notation used here, μ_a is the apparent viscosity of a non-Newtonian fluid at shear rate $\dot{\gamma}$, whereas μ represents a Newtonian coefficient of viscosity.

In the simple shear flow of Fig. 5.1 the shear rate in the fluid can be altered by changing either the separation of the plates or the velocity of the moving plate. For a non-Newtonian fluid the ratio $\tau a/v = \mu_a$ would not be constant, and would depend on the shear rate $\dot{\gamma} = v/a$, whereas for a Newtonian fluid $\tau a/v = \mu$ would be independent of $\dot{\gamma}$. This shear-dependent behaviour may be desirable in the formulation of a food product and is described in the following section.

5.1 Characteristics of non-Newtonian fluids

The characteristics of fluid flow behaviour described in this section are divided into a number of categories:

1. time-independent behaviour, in which the apparent viscosity is independent of the duration or previous history of the deformation;
2. time-dependent viscous behaviour, in which the viscosity changes with time of deformation, but the fluid exhibits no elastic effects; and
3. linear viscoelastic behaviour, in which the fluid exhibits some of the characteristics of a viscous liquid and some of those of an elastic solid.

These characteristics of non-Newtonian materials are discussed in terms of simple viscometric flows, such as the simple shear flow shown in Fig. 5.1. The final discussion in this section considers extensional flows, which involve no shearing, and it will be seen that again food materials exhibit different characteristics from those of Newtonian fluids.

5.1.1 Time-independent shear-thinning and shear-thickening fluids

The range of shear rates that a food fluid may experience during manufacture and consumption is large. For example, Table 5.1 shows shear rates for some typical operations (adapted from Barnes *et al.*, 1989), covering ten orders of magnitude.

In each operation the same fluid is expected to behave in a quite different manner. For example, during spreading the fluid should have a low apparent viscosity, but during chewing or swallowing it should have a higher value of μ_a, which gives a better mouthfeel. This is a fluid that exhibits **shear-thinning** behaviour, in which the viscosity decreases with increasing shear rate. Examples of such fluids are fruit purées, chocolate and meat pastes.

Figure 5.3 shows typical shear-thinning behaviour of a non-Newtonian fluid. At rest, the fluid has a microstructure (due either to interactions between particles within the fluid or to entanglement of macromolecules) that, as the fluid is sheared, is gradually broken down. In some cases the rheological behaviour is found to be independent of time, which means that this breakdown must be reversible, such that the structure is able to reform: that is, under steady shear conditions, time-independent non-Newtonian behaviour is a result of an equilibrium between the structural breakdown and reformation processes. As the shear rate increases, the equilibrium number of interactions or entanglements decreases, resulting in a lower apparent viscosity. This also means that when the rate of strain is decreased, a higher apparent viscosity is obtained as the structure recovers.

For the typical shear-thinning fluid of Fig. 5.3 there are two regions of Newtonian behaviour in which the viscosity is approximately constant, plus a region of decreasing, shear-thinning viscosity. Commonly, the shear-thinning region spans several decades of shear rate. The zero shear stress viscosity μ_0 corresponds to the viscosity of the fully structured fluid, whereas the high shear rate viscosity μ_∞ corresponds to that of the base fluid: that is, after all the structure has been broken down.

Table 5.1 Typical shear rates for food operations

Operation	Typical range of $\dot{\gamma}$ (s^{-1})	Examples
Settling of fine suspensions	10^{-6} to 10^{-4}	Salad dressings
Draining under gravity	10^{-1} to 10^{1}	Vegetable oils
Extrusion	10^{0} to 10^{2}	Snack foods, cereals
Pipe flow	10^{0} to 10^{3}	Chocolate, sauces
Chewing and swallowing	10^{1} to 10^{2}	Most foodstuffs!
Mixing or stirring	10^{1} to 10^{3}	Fruit squashes
Spreading	10^{2} to 10^{4}	Margarine, butter

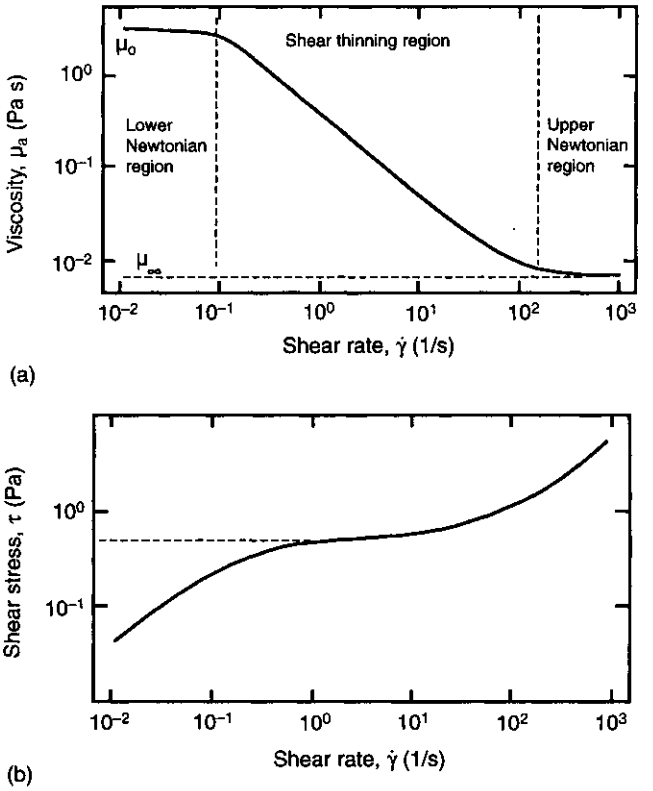

Fig. 5.3 Typical shear-thinning behaviour: (a) viscosity versus shear rate; (b) shear stress versus shear rate.

Cross (1965) developed a first-order model for the rates of breakdown and reformation of the structural interactions in a shear-thinning fluid, resulting in the following constitutive equation:

$$\frac{\mu_a - \mu_\infty}{\mu_0 - \mu_\infty} = \frac{1}{1 + \alpha(\dot{\gamma})^n} \tag{5.5}$$

Equation (5.5) is able to describe the whole range of shear-thinning behaviour including the Newtonian plateau; however, it requires fitting four parameters, μ_∞, μ_0, α and n, to experimental data for μ_a or τ versus $\dot{\gamma}$.

Often, however, it is sufficient to correlate these rheological data for shear stress versus shear rate over a limited range of shear rates using a simple power-law expression. Over the region of shear thinning – that is, for the range of viscosities $\mu_\infty \ll \mu_a \ll \mu_0$ – equation (5.5) becomes approximately

$$\mu_a = \frac{\tau}{\dot{\gamma}} = K(\dot{\gamma})^{n-1} \tag{5.6}$$

or

$$\tau = K(\dot{\gamma})^n \tag{5.7}$$

where K is the **consistency index** and n is the **power-law exponent**. These relationships are compared with Newtonian behaviour in Fig. 5.4.

For shear-thinning fluids the exponent n typically lies in the range 0.2–1, with $n = 1$ corresponding to a Newtonian liquid (compare equations (5.1) and (5.5)). Note that equation (5.7) is simply an engineering representation of the rheological behaviour over a given range of shear rates, and it would be unwise to extrapolate the power law outside this range into either the upper or lower Newtonian regions shown in Fig. 5.3. Usually the power-law equation would be reasonably accurate over two decades of shear rate (Nielsen, 1977).

Some examples of power-law rheological behaviour are given in Table 5.2 (data from Steffe, 1992). The power-law index gives a simple measure of the degree to which the fluid is non-Newtonian. For example, a value of n close to unity would act almost as a Newtonian fluid, whereas banana

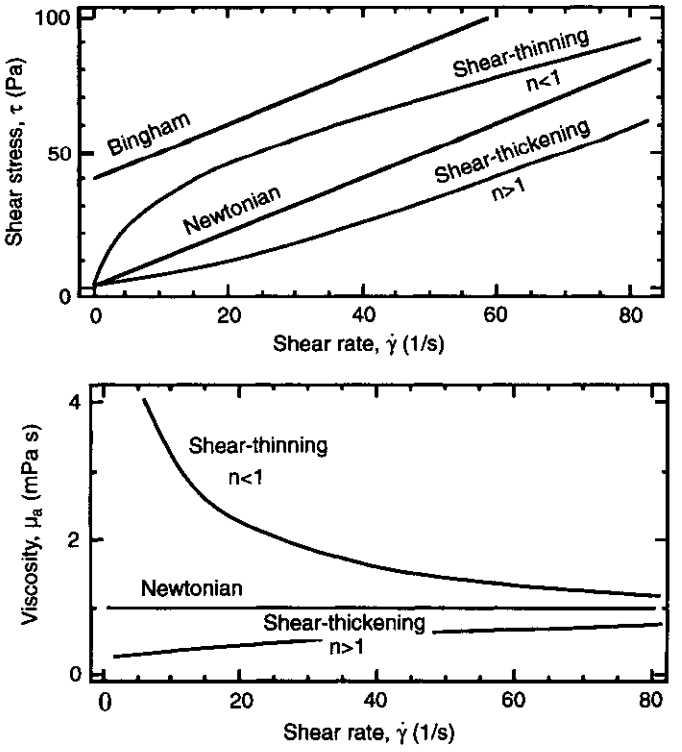

Fig. 5.4 Comparison of some typical Newtonian, shear-thinning and shear-thickening power-law fluids and a Bingham plastic fluid.

Table 5.2 Power-law parameters for various food fluids

Food fluid	T (°C)	n (–)	K (Pa s^n)	Range of $\dot{\gamma}$ (s^{-1})
Banana purée	22	0.28	107.3	28–200
Apple sauce	26	0.45	7.32	0.78–1260
Mayonnaise	25	0.60	4.2	40–1100

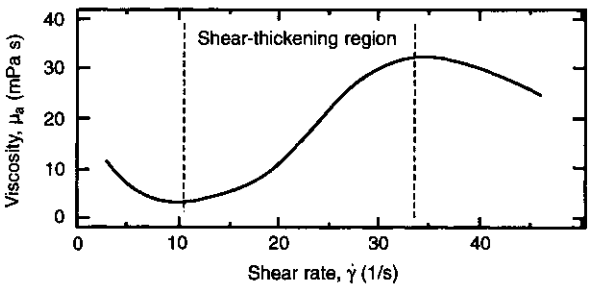

Fig. 5.5 Typical shear-thickening behaviour of a concentrated suspension of non-aggregating particles.

purée, which has a very low index, would exhibit extreme shear-thinning behaviour.

It is also possible for deformation of a fluid to cause rearrangement of its microstructure that results in an **increase** in viscosity with increasing shear rate. **Shear-thickening** fluids are less common than those with shear-thinning behaviour, although most concentrated suspensions of non-aggregating solid particles show some shear-thickening behaviour, given the correct conditions. For example, cornflour pastes and some honeys exhibit shear-thickening behaviour (Steffe, 1992). The explanation offered by Reynolds (1885) is that at rest the voidage fraction of the suspension is at a minimum and there is only just sufficient liquid to fill the voids between particles. At low shear rates the liquid lubricates the motion of one particle past another and the apparent viscosity is small. However, at larger shear rates the dense packing of the material is broken up, and the suspension dilates (the voidage fraction increases). There is now insufficient liquid to lubricate each particle and the apparent viscosity of the particulate mixture increases.

Figure 5.5 shows typical shear-thickening behaviour for a concentrated suspension of particles. Note that there is some shear-thinning behaviour at low shear rates and that shear thickening occurs over less than one decade of $\dot{\gamma}$. In this region, shear-thickening fluids can also be represented by the power law of equation (5.5), but with an exponent of $n > 1$ (see Fig. 5.4).

The next class of non-Newtonian fluids to be considered is **Bingham plastic fluids**, which appear to require a yield shear stress τ_y to be exceeded before fluid deformation takes place: that is, they contain a sufficiently rigid (solid-like) structure that any stress less than the yield stress can be resisted and no continuous motion results. Below the yield stress the material behaves as an elastic solid and stores energy at small strains; at stresses above the yield stress the structure disintegrates and the fluid deforms as a Newtonian fluid under an applied stress $\tau - \tau_y$. The constitutive equation for these fluids is

$$\tau = \tau_y + \mu\dot{\gamma} \qquad \tau > \tau_y$$

and

$$\dot{\gamma} = 0 \qquad \tau < \tau_y \tag{5.8}$$

and they have the stress–strain rate relationship shown in Fig. 5.4. As the Bingham fluid acts as an elastic solid for $\tau < \tau_y$, then it may be more appropriate to write the constitutive equation as

$$\tau = \tau_y + \mu\dot{\gamma} \qquad \tau > \tau_y$$

and

$$\tau = G\gamma \qquad \tau < \tau_y \tag{5.9}$$

where G is a shear modulus for elastic deformation (analogous to Hooke's constant for an elastic spring). The concept of a yield stress fluid is useful in many practical engineering applications (see section 5.4), but its existence is dubious; often, viscometric measurements cannot be made at a sufficiently low shear rate to determine whether a yield stress exists, or if there is extreme shear-thinning behaviour and a very large zero shear viscosity, in the limit, $\dot{\gamma} \to 0$. Figure 5.3(b) shows that if the measurements had been terminated at a strain rate of about $1\,s^{-1}$, then no lower Newtonian region would have been observed and extrapolation to $\dot{\gamma} \to 0$ would suggest that the fluid possessed a yield stress. Barnes *et al.* (1989) discuss this question and conclude that there is no yield stress for dilute solutions and suspensions, but for materials such as ice cream or margarine the flow at very low applied stresses is so slow that motion cannot be observed and there is still some doubt as to the existence of τ_y. For many engineering situations, however, the assumption of Bingham plastic behaviour is a useful approximation, as will be illustrated in section 5.3.1.

The constitutive equations given above for time-independent fluids are the simplest available that characterize shear thinning, shear thickening and yield stress behaviour. Many other empirical equations have been proposed, but their use in solving engineering problems is algebraically more difficult than the simple Cross, power law and Bingham equations. Tanner (1985, p. 15) presents a number of alternative constitutive equations. The

Herschel–Bulkley equation is a useful model for fluids exhibiting both a yield stress and shear-thinning behaviour:

$$\tau = \tau_y + K(\dot{\gamma})^n \tag{5.10}$$

Equation (5.10) now contains three fitted parameters, of which the yield stress is difficult to determine. The most common method of estimating the yield stress is to extrapolate the shear stress versus shear rate curves to $\dot{\gamma} \rightarrow 0$, but this is fraught with the difficulties of obtaining reliable data at low shear rates. Steffe (1992) discusses various other methods of estimating the yield stress. Non-linear regression to find the yield stress gives a result that is highly dependent on the form of the constitutive equation chosen to represent the data.

It is now generally accepted that molten chocolate can be modelled as a **Casson fluid** (Casson, 1959), which obeys a rheological equation of the form

$$(\tau)^{0.5} = (\tau_y)^{0.5} + K(\dot{\gamma})^{0.5} \tag{5.11}$$

The following example, adapted from the calculation presented by Steffe (1992), illustrates the problem of estimating the yield stress and fitting the other model parameters to a given form of constitutive equation.

EXAMPLE 5.1

Using the following rheological data for molten chocolate at 40 °C (Prentice and Huber, 1983) obtain estimates of the yield stress using:

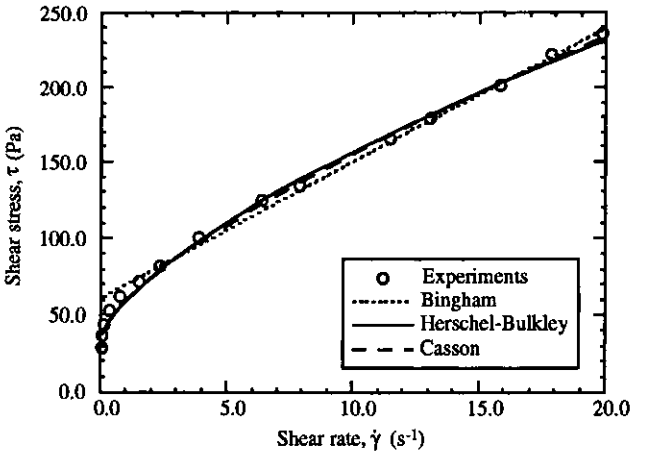

Fig. 5.6 Example 5.1: comparison of regression lines for molten chocolate.

(a) the Bingham plastic equation; (b) the Herschel–Bulkley equation; and (c) the Casson equation.

τ (Pa)	$\dot{\gamma}$ (s^{-1})	τ (Pa)	$\dot{\gamma}$ (s^{-1})
0.099	28.6	6.4	123.8
0.140	35.7	7.9	133.3
0.199	42.8	11.5	164.2
0.390	52.4	13.1	178.5
0.790	61.9	15.9	201.1
1.6	71.4	17.9	221.3
2.4	80.9	19.9	235.6
3.9	100.0		

The following equations were fitted using a non-linear regression method (for the case of the Bingham plastic, only data in the range $\dot{\gamma} = 0.79–19.9\,s^{-1}$ were fitted).

Model	τ_y (Pa)	K (Pa s^n)	n	R^2
Bingham	60.4	8.96	–	0.997
Herschel–Bulkley	33.0	25.5	0.69	0.995
Casson	30.5	2.19	–	0.996

Figure 5.6 shows that the Casson and Herschel–Bulkley equations give an almost indistinguishable fit to the data over the whole range of shear rates, and the two equations predict comparable yield stresses. The Bingham equation considerably overestimates the yield stress, partly because of the assumption of constant viscosity and partly because the low shear rate data were ignored to improve the overall fit of the equation.

5.1.2 Time-dependent non-Newtonian fluids

The fluids discussed in section 5.1.1 show no variation in rheological behaviour with the time that shearing is applied, or with repeated deformation: that is, all of their microstructure is recoverable and breakdown of structural interactions is a reversible process. The rheological behaviour of many real fluids also depends on the duration of the applied shear rate, as well as its magnitude. In this section we shall consider inelastic fluids with time-dependent behaviour; time-dependent effects may also result from the material having some elastic properties, similar to Hookean solids.

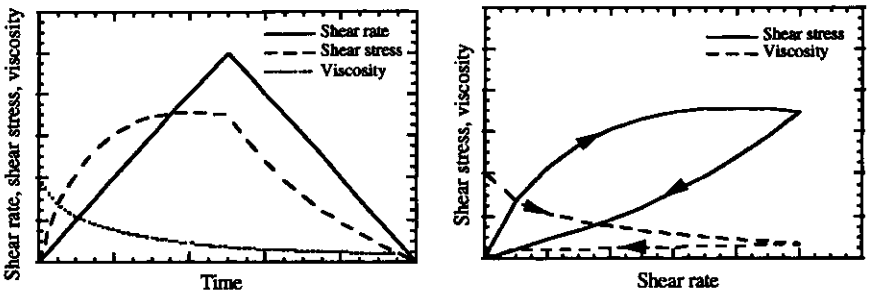

Fig. 5.7 Time-dependent non-Newtonian behaviour. This fluid shows hysteresis, characteristic of thixotropy during a ramp test.

Thixotropic behaviour is obtained from shear-thinning fluids in which no equilibrium is established between the structural breakdown and reformation processes, such that the number of structural interactions decreases continuously with time and the material suffers a permanent change as a result of shearing (for example, starch pastes, gelatins and mayonnaise). Figure 5.7 shows hysteresis loops typical of a thixotropic material for a test in which the shear rate is ramped up and then ramped down over the same time period. For a shear-thinning time-dependent material, initially, the shear stress would increase less than linearly with time. At the midpoint of the ramp test, the shear stress would decrease with time, but the pattern of behaviour would not be a simple reversal of the initial rise. The hysteresis loop for the shear stress is typical of thixotropic materials: here, because the material is both shear-thinning and time-dependent, the viscosity decreases continuously with time.

Similarly, **rheopectic behaviour** can be obtained with shear-thickening fluids in which the apparent viscosity increases with time of deformation. Typically this only occurs at low shear rates, as at higher shear rates the microstructure of the fluid is broken down irreversibly and does not reform.

Constitutive models such as the Herschel–Bulkley equation may be adapted to allow for thixotropic effects by introducing a structural parameter λ (Tiu and Boger, 1974):

$$\tau = \lambda\left(\tau_y + K\left(\dot{\gamma}\right)^n\right) \tag{5.12}$$

The structural parameter has a value $\lambda = 1$ at $t = 0$ and may be described by a second-order decay equation:

$$\frac{d\lambda}{dt} = -k_1\left(\lambda - \lambda_e\right) \quad \text{for} \quad \lambda > \lambda_e \tag{5.13}$$

where λ_e is the final value for complete breakdown of the structure and k_1 is a rate constant that depends on the shear rate. Experiments in which the

fluid is sheared at various constant shear rates may be used to find values of k_1, λ_e, τ_y, K and n; Tiu and Boger (1974) describe these methods applied to a study of the thixotropic behaviour of mayonnaise.

5.1.3 Linear viscoelastic fluids

It was noted in the introduction that complex, structured fluids, such as foodstuffs, behave neither as pure Newtonian liquids, nor as Hookean solids: that is, they simultaneously show viscous and elastic behaviour, and hence are known as **viscoelastic fluids**. A Hookean solid behaves as a perfect spring, such that the shear stress (or force) applied is proportional to the shear strain (or extension). Many polymeric liquids deform in a viscoelastic way; their long chain molecules interact, forming chemical or physical cross-links. A deformation of one part of the fluid is transmitted throughout space to all other entangled chains and the fluid shows some elastic properties. These interactions can give rise to elasticity within the polymer network, large elongational viscosities (see section 5.1.5) and normal stress differences (see section 5.1.4), as well as shear-thinning behaviour. Viscoelasticity can give rise to a variety of effects: for example, in stirred flows, viscoelasticity can result in rod climbing (the **Weissenberg effect**) and flow reversal, which are described in section 10.4.4; and in extrusion processes die-swell is due to elastic effects (see section 5.1.4).

We begin by describing **linear** viscoelastic materials. By linear we mean that the mathematical principle of superposition can be applied to the system. The conditions required are:

1. the stress response of the material is proportional to the magnitude of the applied strain; and
2. the stress response is invariant to time translation; delaying the application of the strain signal by a time T results in the same measured stress, but also delayed by a time T.

These conditions are only likely to be satisfied by small strain deformations; non-linear behaviour would result from large strains.

Before we discuss methods of measuring this type of time-dependent response to deformation it is useful to examine a simple analogue model for linear viscoelastic behaviour. It is convenient to suppose that the fluid

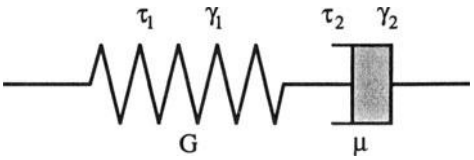

Fig. 5.8 A series-coupled spring and dashpot model: a single Maxwell element.

can be represented by elements exhibiting purely viscous and purely elastic behaviour. Appendix 5.A gives the derivation of a linear Maxwell viscoelastic material, comprising a series-coupled Hookean spring and Newtonian dashpot, as shown in Fig. 5.8. Here the spring has a shear modulus G and the dashpot contains fluid with viscosity μ. For the series combination shown, the shear stress in each element is the same, but the total shear strain is the sum of the shear strain in each part.

This model results in the linear differential equation (Appendix 5.A),

$$\frac{d\tau}{dt} + \frac{\tau}{\lambda} = G\dot{\gamma} \tag{5.14}$$

where $\lambda = \mu/G$ is the **relaxation time**. Equation (5.14) may be integrated to give

$$\tau(t) = G\int_{-\infty}^{t} \exp\left(-\frac{t-t'}{\lambda}\right)\dot{\gamma}(t')\,dt' \tag{5.15}$$

showing that the shear stress at time t depends on the previous history of the deformation $\dot{\gamma}(t')$ from $t' = -\infty$ to $t' = t$. (t' is a dummy integration variable and is used to distinguish the present time t from all previous times t'.)

The choice of a single spring in series with a single dashpot is simple but quite arbitrary; many other combinations of springs and dashpots have been formulated to give different viscoelastic responses. For example, the **Voigt model** comprises a parallel-coupled spring and dashpot combination. In practice, a single Maxwell element does not give a satisfactory representation of linear viscoelastic behaviour. However, because of the linear nature of equation (5.14) it is possible to superimpose a number of solutions from n parallel Maxwell elements (Fig. 5.9), each with its own relaxation time λ_i and shear modulus G_i to give the generalized model

$$\tau(t) = \sum_{i=1}^{n} G_i \int_{-\infty}^{t} \exp\left(-\frac{t-t'}{\lambda_i}\right)\dot{\gamma}(t')\,dt' \tag{5.16}$$

We can now apply this integral constitutive equation to predict linear viscoelastic behaviour for a number of deformation histories. Initially we consider a steady shear rate applied to a single Maxwell element:

$$\dot{\gamma}(t') = \dot{\gamma}_0 \qquad -\infty < t' < t \tag{5.17}$$

Substitution of equation (5.17) into equation (5.15) and integration gives

$$\tau(t) = \mu\dot{\gamma}_0 \tag{5.18}$$

So, the linear viscoelastic fluid behaves as a simple Newtonian under steady shear. This is one of the drawbacks of using linear models, as many real viscoelastic food fluids also exhibit shear-thinning behaviour, and the ratio $\tau/\dot{\gamma}$ should decrease with increasing shear rate: non-linear models

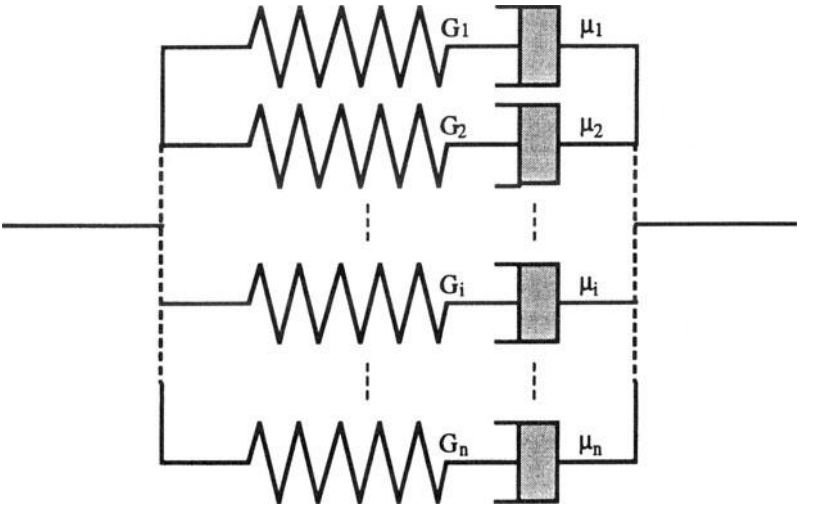

Fig. 5.9 An analogue model of a linear viscoelastic fluid: n parallel Maxwell elements.

are required to represent this behaviour, but are beyond the scope of this book.

Now let us consider the cessation of the steady shear at time $t' = 0$:

$$\begin{aligned} \dot{\gamma}(t') &= \dot{\gamma}_0 \qquad t' < 0 \\ \dot{\gamma}(t') &= 0 \qquad t' \geqslant 0 \end{aligned} \tag{5.19}$$

Substituting equation (5.19) into equation (5.15) and integrating yields

$$\begin{aligned} \tau(t) &= \mu \dot{\gamma}_0 && t < 0 \\ \tau(t) &= \mu \dot{\gamma}_0 \exp\left(-\frac{t}{\lambda}\right) && t \geqslant 0 \end{aligned} \tag{5.20}$$

The plot of equation (5.20) in Fig. 5.10 shows that even after deformation has stopped the fluid is able to sustain shear stresses, but that they decay exponentially to zero with a relaxation time λ.

This viscoelastic behaviour is quite different from that of a Newtonian fluid and is due to the existence of elastically loaded molecular entanglements, even after fluid motion has ceased. Figure 5.10 also shows the behaviour of (i) a Newtonian fluid where the shear stress drops to zero as soon as the rate of deformation ceases, and (ii) an elastic solid where the shear stress remains constant at the value at the cessation of shearing, which corresponds to $G\gamma$, where γ is the final strain.

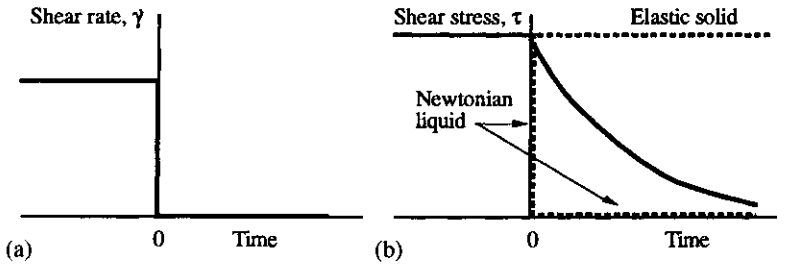

Fig. 5.10 Stress relaxation following the cessation of steady shear.

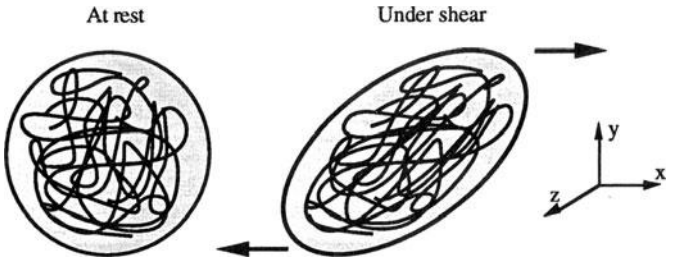

Fig. 5.11 Normal stresses generated by anisotropic structure under shear.

5.1.4 Normal stress differences

One part of the definition of a Newtonian fluid is that the normal stress differences are zero in simple shear flow (see equation (5.2)):

$$N_1 = \sigma_{xx} - \sigma_{yy} = 0$$

and

$$N_2 = \sigma_{yy} - \sigma_{zz} = 0 \tag{5.21}$$

For linear viscoelastic fluids these normal stresses are also zero; they arise as second-order terms in $\dot{\gamma}$ and are associated with **non-linear viscoelastic effects**. Physically, the explanation for these normal stress differences is that at high shear rates the microstructure of the fluid becomes anisotropic (direction-dependent). Consider the schematic of a dilute polymer solution in Fig. 5.11: at rest the molecular envelope may be taken to be spherical and contains a number of entangled polymer chains, which are randomly oriented in space. Under shear the envelope deforms to an ellipsoidal shape and the molecules are stretched and partially aligned in the x direction.

The restoring forces in this deformed microstructure are anisotropic, such that usually the largest normal stress would be σ_{xx}: that is, in the

direction of the flow. This leads to a positive first normal stress difference, $N_1 = \sigma_{xx} - \sigma_{yy} > 0$; generally the second normal stress difference $N_2 = \sigma_{yy} - \sigma_{zz}$ is much smaller than the first, $|N_2| \ll N_1$, and is of secondary importance. Over a range of strain rates the first normal stress difference may be written as a power-law function of $\dot{\gamma}$:

$$N_1 = A(\dot{\gamma})^m \tag{5.22}$$

and it is not unusual for the ratio N_1/τ to be greater than 1, indicating a highly elastic state (Barnes *et al.*, 1989).

The existence of normal stress differences can give unusual flow effects in industrial applications (see also section 10.4.4). For instance, a rod rotating in a Newtonian fluid would cause a depression of the free surface because of formation of a surface vortex. In a viscoelastic fluid the normal stress differences causes a phenomenon known as the **Weissenberg effect**, in which the fluid actually climbs the rotating rod. Normal stress effects can also cause **reversal of the flow pattern** direction in impeller-driven tanks. In extrusion processes the phenomenon of **die swell** is due to the relaxation of normal stresses on exit from the die, and can give an increase in diameter of the extrudate by a factor of 2 or 3.

5.1.5 Elongational viscosity effects

Consider the element of fluid shown in Fig. 5.12, which is being stretched along its x axis at a constant rate $\partial v_x/\partial x = \dot{\varepsilon}$. In a purely elongational flow all the shear stresses are zero, $\tau_{xy} = \tau_{xz} = \tau_{yz} = 0$, and the normal stress components are equal in the y and z directions, $\sigma_{yy} = \sigma_{zz}$ (by symmetry). If the fluid is incompressible, its volume must be conserved, so that for an axisymmetric flow

$$\frac{\partial v_x}{\partial x} = \dot{\varepsilon} \qquad \text{and} \qquad \frac{\partial v_y}{\partial y} = \frac{\partial v_z}{\partial z} = -\frac{\dot{\varepsilon}}{2} \tag{5.23}$$

(see Tritton (1988) for an explanation of the continuity equation for three-dimensional flow).

The normal viscous stress differences are given by

$$\sigma_{xx} - \sigma_{yy} = \sigma_{xx} - \sigma_{zz} = \mu_E \dot{\varepsilon} \tag{5.24}$$

where μ_E is the **elongational viscosity**. In general, the elongational viscosity depends on the elongational strain rate $\dot{\varepsilon}$ and time. For a Newtonian fluid in uniaxial extensional flow the ratio of extensional to the shear viscosity is constant, $\mu_E/\mu = 3$, but for non-Newtonian fluids μ_E may increase (tension thickening) or decrease (tension thinning) with increasing $\dot{\varepsilon}$. Moreover, non-Newtonian fluids can have very large ratios of elongational to shear viscosity (orders of magnitude greater than for Newtonian fluids). These effects become very important in flows with converging streamlines (as shown in

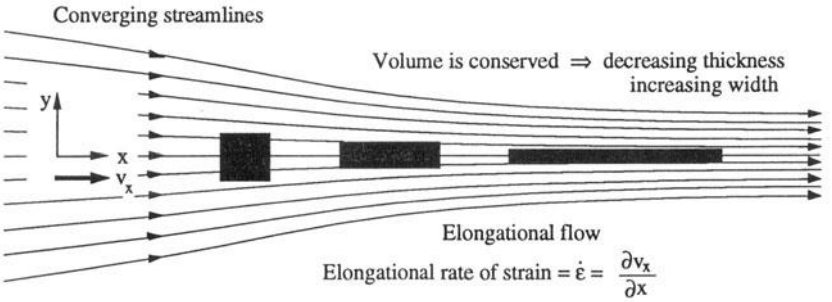

Fig. 5.12 An element of fluid undergoing elongational flow.

Fig. 5.12), where elongation of fluid elements takes place. For example, in the entrances to dies during extrusion, the flow is substantially changed by having a large elongational viscosity. Elongational flows also take place in valve homogenizers (used for emulsion formation), where the elongational strain is extremely efficient at causing droplet breakup. One of the more remarkable demonstrations of the effect of a large elongational viscosity is the open siphon experiment in which fluid can be sucked up from a reservoir, even though the tube is above the liquid free surface.

5.2 Viscometric flows

In the previous section we discussed some of the characteristics of non-Newtonian fluids under flow conditions in which either the rate of strain $\dot{\gamma}$ or the shear stress τ was controlled. In this section we shall examine the types of equipment suited to generating these flows and their use in determining rheological parameters in the constitutive equations. The flows described are known as **viscometric** as they are simple and well defined and are usually designed so that there is a controlled shear rate in a single direction. These flows would always be in the laminar flow regime (see Chapter 2). There are numerous devices for measuring the rheological behaviour of fluids, but here we shall concentrate only on those in which the rate of strain may be directly controlled. Devices such as the falling sphere or U-tube viscometer do not allow application of a prescribed shear rate and are really only suitable for use with Newtonian fluids. Many books (e.g. Steffe, 1992) describe the application of these measurement devices to Newtonian food fluids.

5.2.1 Measurement of shear viscosity: the concentric cylinder viscometer

Figure 5.1 shows an idealized simple shear flow between two flat plates, of which one is stationary and the other moves at a velocity v. The same flow

field can be generated using the narrow-gap, concentric cylinder device shown in Fig. 5.13.

If the gap width $r_2 - r_1$ is small compared with the inner radius r_1, then the shear rate between the cylinders is approximately uniform and can be controlled by altering the rotational speed ω (rad s^{-1}) of the inner cylinder (see Appendix 5.B)

$$\dot{\gamma} = \frac{\left(2\omega/r^2\right)\left(r_1^2 r_2^2\right)}{\left(r_2^2 - r_1^2\right)} \approx \frac{r_1\omega}{r_2 - r_1} \qquad \text{for} \qquad \frac{r_1}{r_2} > 0.96 \tag{5.25}$$

Thus we shall assume that $\dot{\gamma}$ is independent of r in the narrow gap.

The shear stress in the fluid can be deduced from a measurement of the torque Γ_1 on the inner cylinder:

$$\tau = \frac{\Gamma_1}{2\pi r_1^2 L} \tag{5.26}$$

(Other arrangements in which the outer cylinder rotates with the inner stationary, or in which the torque on the outside cylinder is measured, are also possible.) The design of these viscometers usually incorporates a recessed top and bottom to the inner cylinder so that the fluid shear stress acts only on the side walls. Using the definition of the apparent viscosity, given in equation (5.4), then (see Appendix 5.B for full analysis)

$$\mu_a(\dot{\gamma}) = \frac{\tau}{\dot{\gamma}} = \frac{\Gamma_1}{4\pi\omega L}\left[\frac{1}{r_1^2} - \frac{1}{r_2^2}\right] \tag{5.27}$$

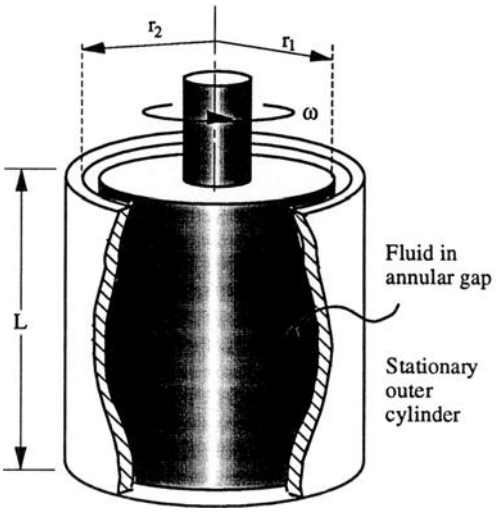

Fig. 5.13 Geometry of a concentric cylinder viscometer.

For food materials, in particular with suspended solid particles, it may not be possible to use a narrow-gap device, in which case the shear rate would vary with radius. Kreiger and Maron (1954) showed that for a power-law fluid the shear rate at the inner cylinder is

$$\dot{\gamma}_1 = \frac{2\omega}{n\left(1-\left(r_1/r_2\right)^{2/n}\right)} \tag{5.28}$$

and the viscosity at this shear rate is

$$\mu_a\left(\dot{\gamma}_1\right) = \frac{\Gamma_1 n\left(1-\left(r_1/r_2\right)^{2/n}\right)}{4\pi r_1^2 L\omega} \tag{5.29}$$

For a power-law fluid, the shear stress on the inner cylinder is

$$\tau_1 = K\left(\dot{\gamma}\right)^n = K\left[\frac{2\omega}{n\left(1-\left(r_1/r_2\right)^{2/n}\right)}\right]^n \tag{5.30}$$

and taking logs of equation (5.30) gives

$$\ln\left(\tau_1\right) = n\ln\omega + n\ln\left[K^{1/n}\frac{2}{n\left(1-\left(r_1/r_2\right)^{2/n}\right)}\right] \tag{5.31}$$

The second term on the right-hand side of equation (5.31) is independent of rotational speed, so a plot of $\ln(\tau_1)$ versus $\ln\omega$ has a slope n and an intercept related to the consistency index K. An alternative form of analysis is given in Example 5.2 below.

With wide-gap devices there is a danger that above a critical rotational speed **Taylor vortices**, a form of flow instability, may form in the gap, disturbing the simple shear flow pattern (see Tritton, 1988, p. 260). Measurements from such an unstable flow would not be performed in a simple shear field and would not yield useful information.

EXAMPLE 5.2

A concentric cylinder Couette viscometer is used to measure the rheological properties of a tomato juice. The inner cylinder rotates at a speed of N *revolutions per second; the torque on the inner cylinder is*

measured. The inner cylinder has a radius $r_1 = 0.025\,m$ *and length 0.04 m. The outer cylinder has a radius* $r_2 = 0.026\,m$. *Find an appropriate time-independent constitutive equation that represents the fluid rheology over the range of applied shear rates.*

N (rps)	0.01	0.02	0.05	0.1	0.2	0.5	1	2	5
Γ_1 ($Nm \times 10^{-3}$)	2.37	3.58	5.72	7.80	1.04	1.49	1.97	2.64	4.09

Convert the above data to strain rates and shear stresses using, respectively, equations (5.25) and (5.26). Note that the ratio $r_1/r_2 = 0.96$, so the approximate form of equation (5.25) will suffice, and the shear rate may be assumed to be constant across the annular gap. Calculation of the apparent viscosity at each rotational speed shows that indeed this material exhibits shear-thinning behaviour.

ω ($rad\,s^{-1}$)	0.063	0.13	0.31	0.63	1.26	3.14	6.28	12.57	31.42
$\dot{\gamma}$ (s^{-1})	1.57	3.14	7.85	15.7	31.4	78.5	157.0	314.1	785.3
τ ($N\,m^{-2}$)	1.51	2.28	3.64	4.97	6.61	9.48	12.51	16.80	26.02
μ_a ($Pa\,s$)	0.959	0.725	0.464	0.316	0.210	0.121	0.080	0.053	0.033

Plotting the shear stress versus the shear rate on a log–log plot reveals that a power-law model would be suitable (Fig. 5.14). Linear regression of the data gives that

$$\tau = 1.37\dot{\gamma}^{0.44} \quad \text{for} \quad 1.0\,s^{-1} < \dot{\gamma} < 1000\,s^{-1}$$

$$= 1.37\,\dot{\gamma}^{0.44} \quad \text{for } 1.0\,s^{-1} < \dot{\gamma} < 1000\,s^{-1}.$$

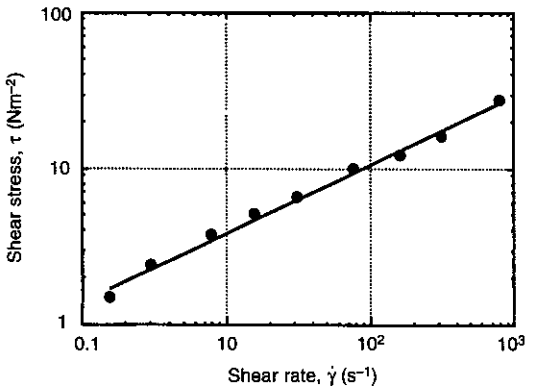

Fig. 5.14 Log–log plot for shear stress versus shear rate for a power-law fluid.

Final remark: the data for this example was 'artificially' created from the Cross model, using the form

$$\frac{\mu_a - 0.01}{0.2 - 0.01} = \frac{1}{1 + 0.8\,(\dot{\gamma})^{0.7}}$$

illustrating that equation (5.5) reduces approximately to the simple power-law form over the range of shear rates where shear-thinning behaviour is exhibited. However, extrapolation of the power-law outside this range of $\dot{\gamma}$ could give erroneous results.

5.2.2 *Measurement of shear viscosity: capillary flow viscometers*

For Newtonian fluids in laminar flow the pressure drop per unit length of capillary, $\Delta P/L$, is related to the volumetric flowrate w_L by the Hagen–Poiseuille equation (equation (2.37)) and the viscosity may be calculated from

$$\mu = \frac{\Delta P \pi a^4}{8 L w_L} \tag{5.32}$$

Unfortunately, the shear rate within the fluid depends on radial position:

$$\dot{\gamma} = -\frac{\Delta P r}{2 L \mu} \tag{5.33}$$

and so this device is more difficult to use with non-Newtonian fluids. Walters (1975) shows that the shear rate at the wall ($r = a$) is given by

$$\dot{\gamma}_w = \frac{4 w_L}{\pi a^3}\left(\frac{3}{4} + \frac{1}{4}\frac{\mathrm{d}\ln w_L}{\mathrm{d}\ln \tau_w}\right) \tag{5.34}$$

where the term in the bracket is known as the **Rabinowitch correction**. The wall shear stress τ_w is related to the pressure gradient by

$$\tau_w = \frac{a}{2}\frac{\Delta P}{L} \tag{5.35}$$

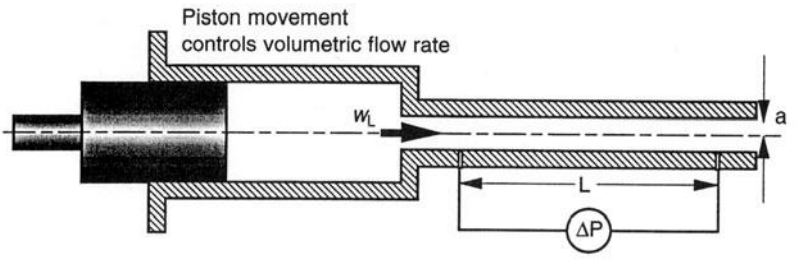

Fig. 5.15 Capillary flow viscometer.

so that the viscosity at the wall shear rate is

$$\mu_a(\dot{\gamma}_w) = \frac{\pi a^4 \Delta P/L}{8w_L\left(\frac{3}{4} + \frac{1}{4}\frac{d\ln w_L}{d\ln \tau_w}\right)} \tag{5.36}$$

Thus by measuring $\Delta P/L$ versus w_L the apparent viscosity of the fluid may be deduced. Additional problems associated with entrance effects are discussed by Mackley (1988) and Steffe (1992). Example 5.3 below shows how these equations may be used to characterize data from food fluids in capillary flow viscometers.

EXAMPLE 5.3

The following data were collected for orange juice concentrate in a 2 mm diameter capillary viscometer with a length of 0.25 m. Find the power-law index and consistency index from these data.

Raw data		Calculated data	
w_L ($m^3 s^{-1}$)	ΔP (Pa)	τ_w (Pa)	$\dot{\gamma}_w$
1.0×10^{-7}	1.75×10^4	34.9	135.8
2.0×10^{-7}	3.03×10^4	60.5	271.6
3.0×10^{-7}	4.13×10^4	82.5	407.4
4.0×10^{-7}	5.27×10^4	105.3	543.1
5.0×10^{-7}	6.10×10^4	122.0	678.9
6.0×10^{-7}	7.18×10^4	143.5	814.7
7.0×10^{-7}	8.16×10^4	163.1	950.5
8.0×10^{-7}	9.26×10^4	185.2	1086.3
9.0×10^{-7}	9.86×10^4	197.2	1222.1
1.0×10^{-6}	1.06×10^5	212.0	1357.8

The tube length to diameter ratio is very large, so that end effects can be neglected. The first step is to calculate the wall shear stress, τ_w from equation (5.35) and then to plot w_L versus τ_w on a log–log plot (Fig. 5.16(a)). The slope of this line gives the Rabinowitch correction

$$\frac{d\ln w_L}{d\ln \tau_w} = 1.266$$

This allows the wall shear rate to be calculated from equation (5.34); a further regression of the wall shear stress versus the wall shear rate on log–log axes (Fig. 5.16(b)) gives the power law exponent and consistency index as

$$n = 0.79 \quad \text{and} \quad K = 0.72\,\text{Pa}\,\text{s}^n$$

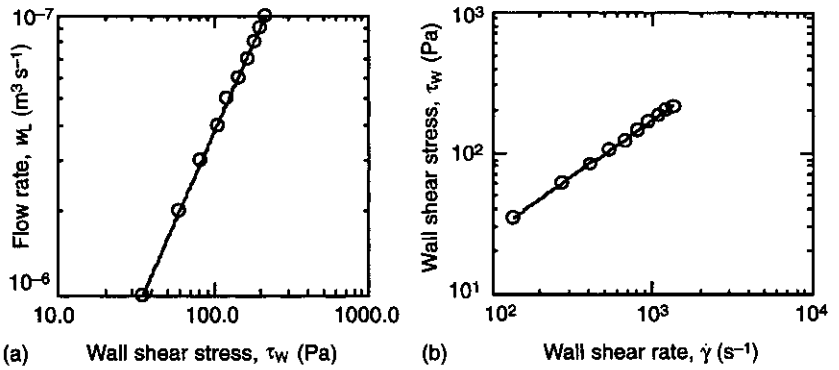

Fig. 5.16 Example 5.3: plot (a) is used to find the Rabinowitch correction and plot (b) is used to find the power-law parameters.

5.2.3 Cone and plate viscometers

Figure 5.17 shows the geometric arrangement of this viscometer: the fluid is held between a cone and a plate; the plate rotates at an angular frequency, ω (rad s^{-1}), while the cone remains stationary; the torque Γ on the cone is measured using a transducer. Provided that the cone angle θ is small (<4°), then the shear rate in the liquid is uniform and given by

$$\dot{\gamma} = \frac{\omega}{\tan\theta} \tag{5.37}$$

The shear stress is given by

$$\tau = \frac{3\Gamma}{2\pi R^3} \tag{5.38}$$

and so the viscosity may be calculated from (see Appendix 5.C for details)

$$\mu_a(\dot{\gamma}) = \frac{3\Gamma\tan\theta}{2\pi R^3\omega} \tag{5.39}$$

5.2.4 Parallel plate viscometer

The parallel plate viscometer (see Fig. 5.17) operates in a similar way to the cone and plate device, except that the shear rate in the gap is no longer uniform and analysis for non-Newtonian fluids becomes more difficult (see Barnes *et al.*, 1989).

5.2.5 Measurement of viscoelastic properties

Cone and plate and parallel plate viscometers are suitable for determining the shear viscosity of time-independent non-Newtonian fluids, but their

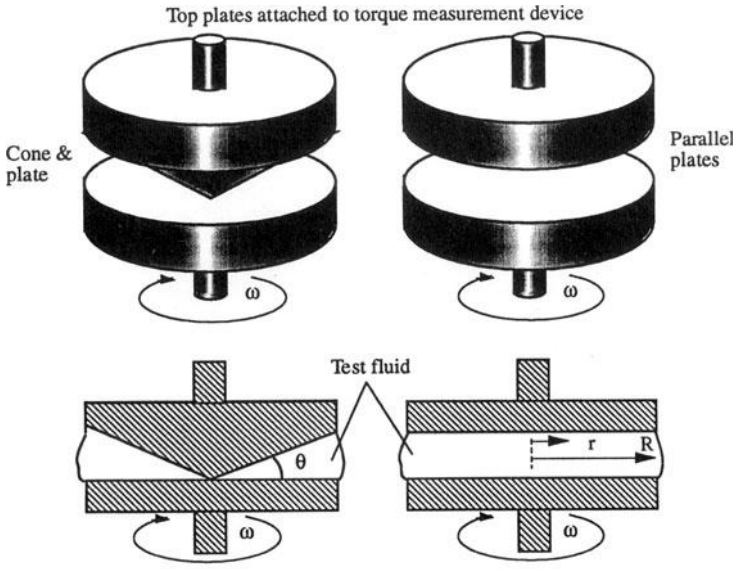

Fig. 5.17 Cone and plate and parallel plate viscometers.

main advantage is in oscillatory mode, for the measurement of viscoelastic properties. The lower plate is made to oscillate at a frequency ω (rad s^{-1}), giving a sinusoidally varying strain in the fluid, with a maximum amplitude of γ_o:

$$\gamma = \gamma_o \sin\omega t \tag{5.40}$$

Differentiating equation (5.40) with respect to time gives the strain rate as

$$\dot{\gamma} = \frac{d\gamma}{dt} = \dot{\gamma}_o \omega \cos\omega t \tag{5.41}$$

The shear stress, deduced from torque measurements, on the upper plate also varies sinusoidally, at the same frequency as the strain oscillation, but shifted out of phase by an angle δ:

$$\tau = \tau_o \sin(\omega t + \delta) \tag{5.42}$$

or

$$\tau = \tau_o \cos\delta \sin(\omega t) + \tau_o \sin\delta \cos(\omega t) \tag{5.43}$$

where τ_o is the maximum shear stress. At this point it is worth noting that if the material was a Hookean elastic solid, the angle δ would be zero as the shear stress would be in phase with the strain oscillation. Hooke's law for a solid material is

$$\tau = G\gamma = G\gamma_o \sin(\omega t) \tag{5.44}$$

where G is the shear modulus and γ is the shear strain.

However, if the material was a Newtonian fluid, the shear stress would be $\pi/2$ radians out of phase with the strain oscillation as

$$\tau = \mu\dot{\gamma} = \mu\gamma_o\omega\cos(\omega t)$$

$$\Rightarrow \quad \tau = \mu\gamma_o\omega\sin\left(\omega t + \frac{\pi}{2}\right) \tag{5.45}$$

To characterize the elastic and viscous components, we define the **elastic storage modulus** G' from the in-phase component of the stress in equation (5.43):

$$G' = \frac{\tau_o}{\gamma_o}\cos\delta \tag{5.46}$$

and the **loss modulus** G'' from the out-of-phase component of stress:

$$G'' = \frac{\tau_o}{\gamma_o}\sin\delta \tag{5.47}$$

For a perfectly elastic Hookean solid the shear stress ($\delta = 0$) and shear strain would be related by equation (5.44), giving an elastic storage modulus of $G' = G$ and a loss modulus of $G'' = 0$. Compare this with the response of a Newtonian viscous liquid ($\delta = \pi/2$), which has an elastic storage modulus of $G' = 0$ and a loss modulus of $G'' = \mu\omega$. Thus the relative values of the moduli G' and G'' from oscillatory tests yields information about the degree of elastic and viscous behaviour exhibited by the food material.

We can also define a **complex viscosity** μ^*, the magnitude of which is

$$|\mu^*| = \frac{\left(G'^2 + G''^2\right)^{1/2}}{\omega} \tag{5.48}$$

This is akin to the apparent viscosity defined in equation (5.4). These three parameters may then be used to describe the viscoelastic characteristics of a fluid. For most polymers, structured fluids and foodstuffs, G', G'' and $|\mu^*|$ are all functions of the oscillation frequency, and possibly also the strain amplitude γ_o and time.

The bulk and storage moduli may now be examined for a simple linear viscoelastic fluid, such as that discussed in section 5.1.3. For a single series-coupled Maxwell element the storage and loss moduli and complex viscosity are given by (see Appendix 5.A)

$$G' = \frac{G\lambda^2\omega^2}{\left(1 + \lambda^2\omega^2\right)} \tag{5.49}$$

$$G'' = \frac{G\lambda\omega}{\left(1+\lambda^2\omega^2\right)} \tag{5.50}$$

$$\left|\mu^*\right| = \frac{G\lambda}{\left(1+\lambda^2\omega^2\right)^{1/2}} \tag{5.51}$$

Figure 5.18 shows a schematic plot of these parameters for a single element, which can be compared with Figs 5.19 and 5.20, which show some typical strain and frequency sweeps for a polymeric foodstuff and a gel or suspension foodstuff. The Maxwell element represents linear viscoelastic behaviour in which G' and G'' are independent of the magnitude of the strain γ_o. G' is a monotonically increasing function of dimensionless frequency $\omega\lambda$, which becomes constant at high dimensionless frequency, and G'' has a maximum at $\omega\lambda = 1$. Figure 5.18 shows that at low dimensionless frequencies (slow deformation rates) the behaviour is viscous in nature ($G' \ll G''$), whereas at high dimensionless frequencies elastic effects dominate ($G' \ll G''$).

Figures 5.19 and 5.20 show that both the polymeric and gel foodstuffs show linear viscoelastic behaviour at low strains (G' and G'' are independent of the magnitude of the maximum strain γ_o), but non-linear response at higher strains. The gel foodstuff (yoghurt, for example) shows four separate regions (Steventon *et al.* 1991):

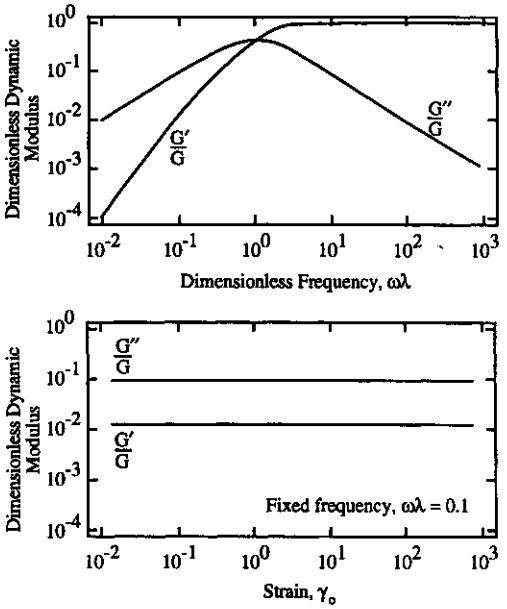

Fig. 5.18 Frequency and strain sweeps for a single Maxwell element.

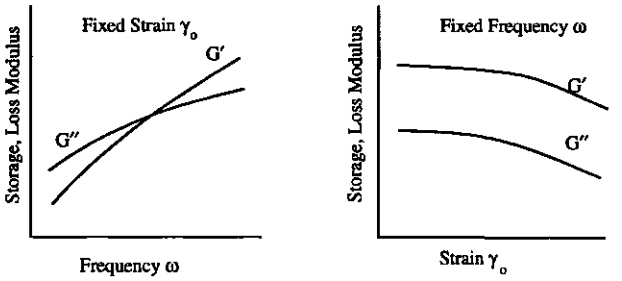

Fig. 5.19 Typical frequency and strain sweeps for a polymeric foodstuff.

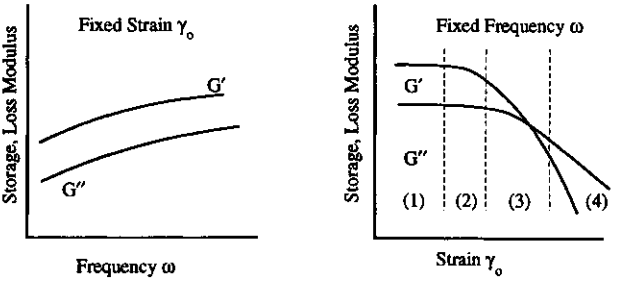

Fig. 5.20 Typical frequency and strain sweeps for a gel or suspension foodstuff.

1. a linear viscoelastic region in which G' and G'' are constant and the material is predominantly elastic ($G' \gg G''$);
2. a non-linear region in which G'' is fairly constant and G' starts to decrease, indicating breakdown of the elastic structure;
3. where G' and G'' cross over after the full elastic structure has been broken and the material becomes more viscous; and
4. where viscous behaviour dominates ($G'' \gg G'$).

It is clear that the single Maxwell element does not correspond to the behaviour of real polymeric foodstuffs. However, many parallel Maxwell elements with time constants λ_i and shear moduli G_i give an improved representation of real frequency-sweep behaviour (see Fig. 5.21) but not of the effect of strain on the loss and storage moduli. For n Maxwell elements the separate solutions of equations (5.49)–(5.51) can simply be added because of the linear nature of the constitutive equation:

$$G' = \sum_{i=1}^{n} \frac{G_i \lambda_i^2 \omega^2}{\left(1 + \lambda_i^2 \omega^2\right)} \tag{5.52}$$

$$G'' = \sum_{i=1}^{n} \frac{G_i \lambda_i \omega}{\left(1 + \lambda_i^2 \omega^2\right)} \tag{5.53}$$

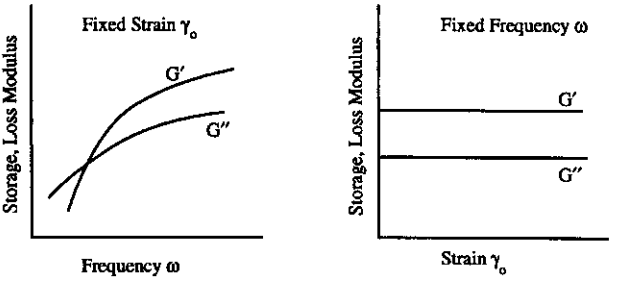

Fig. 5.21 Typical frequency and strain sweeps for n Maxwell elements.

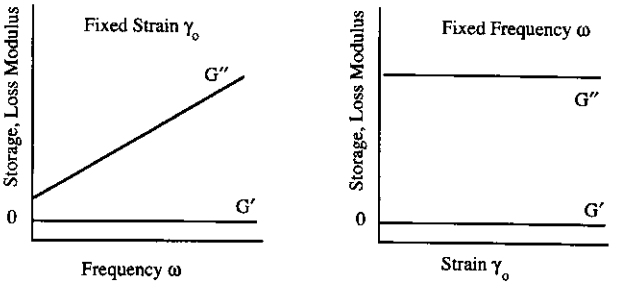

Fig. 5.22 Frequency and strain sweeps for a Newtonian fluid.

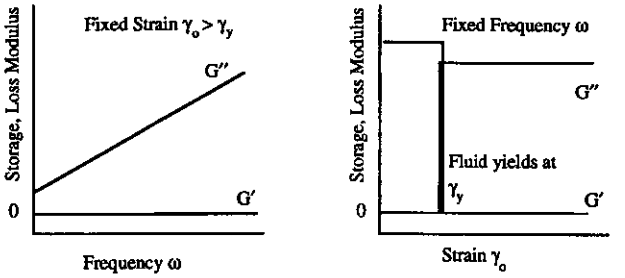

Fig. 5.23 Frequency and strain sweeps for a Bingham plastic.

and

$$|\mu^*| = \sum_{i=1}^{n} \frac{G_i \lambda_i}{\left(1+\lambda_i^2 \omega^2\right)^{1/2}} \tag{5.54}$$

For comparison, the frequency and strain sweeps for Newtonian and Bingham fluids have been included in Figs 5.22 and 5.23. For a Newtonian fluid the storage modulus should be close to zero, whereas the loss modulus

should be proportional to the viscosity of the fluid and to the frequency. Both G' and G'' should be independent of the strain. This can be compared with the Bingham plastic, which exhibits elastic solid behaviour at small strains, and purely viscous behaviour at strains above the elastic limit.

Example 5.4 below shows how data from an oscillatory test in a cone and plate viscometer can be used to derive storage and loss moduli and Maxwell model parameters.

EXAMPLE 5.4

Tomato ketchup was sheared between the cone and plate of an oscillatory rheometer: the cone angle was $\theta = 0.07$ rad (4°) and the plate radius was $R = 12.5$mm. The maximum amplitude of the oscillation was $\phi_o = 0.009$ rad. The data below give the maximum torque Γ_{max} and phase angle δ relative to the oscillatory strain

$$\gamma = \gamma_o \sin \omega t$$

At any radius r the maximum strain is given by the maximum displacement divided by the distance between cone and plate. That is:

$$\gamma_o = \frac{r\phi_o}{r\tan\theta} = \frac{\phi_o}{\tan\theta} = \frac{0.009}{\tan 0.07} = 0.13$$

which is independent of radius and thus the shear stress also should not be a function of r. The torque is given by

$$\Gamma = \int_0^R 2\pi r^2 \tau dr = \frac{2\pi R^3 \tau}{3} \Rightarrow \tau_o = \frac{3\Gamma_{max}}{2\pi R^3}$$

From equations (5.46) and (5.47)

$$G' = \frac{\tau_o}{\gamma_o}\cos\delta \qquad \text{and} \qquad G'' = \frac{\tau_o}{\gamma_o}\sin\delta$$

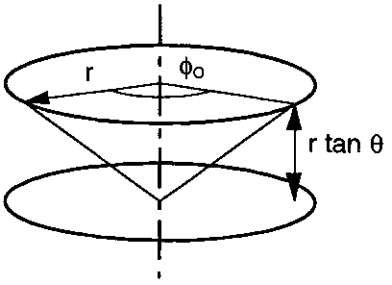

Calculating the storage and loss moduli gives the fifth and sixth columns of the table below.

Raw data			Calculated data		
ω (rad s^{-1})	Γ_{max} (N m)	δ (rad)	τ_o (N m^{-2})	G' (N m^{-2})	G'' (N m^{-2})
0.200	1.69×10^{-4}	0.126	41.23	3.19×10^{2}	4.03×10^{1}
0.600	1.85×10^{-4}	0.142	45.33	3.50×10^{2}	4.98×10^{1}

We shall attempt to use these data to fit a single element Maxwell model of the form

$$G' = \frac{G\lambda^2\omega^2}{(1+\lambda^2\omega^2)}$$

$$G'' = \frac{G\lambda\omega}{(1+\lambda^2\omega^2)}$$

The first data set at $\omega = 0.2\,\text{rad s}^{-1}$ gives $G = 324\,\text{N m}^{-2}$ and $\lambda = 39.6\,\text{s}$, whereas the second data set at $\omega = 0.2\,\text{rad s}^{-1}$ gives $G = 357\,\text{N m}^{-2}$ and $\lambda = 11.7\,\text{s}$, which are not in particularly good agreement. The reasons for this discrepancy are that: (a) a single Maxwell element is not sufficient to characterize the behaviour of most viscoelastic food stuffs; and (b) the maximum strain in this case is 13%, which is likely to be outside the range of linear behaviour.

5.3 Application to engineering problems

Non-Newtonian fluid rheology can lead to quite different flow behaviour from that of Newtonian fluids and has a profound effect on parameters such as pressure drop in pipeline flow, heat and mass transfer, mixing rate (see section 10.4.4) and residence time distribution. Some of the more dramatic observable changes have already been discussed in section 5.1. We shall conclude this chapter by applying some non-Newtonian constitutive equations to the problem of predicting the pressure drop for power-law and Bingham plastic fluids flowing through pipes.

5.3.1 Non-Newtonian pipe flows

As an example we consider flow of a power-law fluid through a round pipe, and we draw on the approach used in section 2.3.2. A force balance on a cylindrical element, as in Fig. 2.11, yields

$$\tau = \frac{r}{2}\frac{dP}{dL} \tag{5.55}$$

where now

$$\tau = K\left(\dot{\gamma}\right)^n = K\left(\frac{dv_x}{dr}\right)^n \tag{5.56}$$

For convenience we shall call the pressure gradient

$$s = -\frac{dP}{dL} = \frac{\Delta P}{L} \tag{5.57}$$

noting that the pressure gradient has a negative value, but that the pressure drop ΔP is treated as being positive. Then

$$\left(\frac{sr}{2K}\right)^{1/n} = \left(\frac{dv_x}{dr}\right) \tag{5.58}$$

Integrating equation (5.58), using the boundary condition that $v_x = 0$ at $r = a$,

$$v_x(r) = \int_a^r \left(\frac{sr}{2K}\right)^{1/n} dr = \left(\frac{s}{2K}\right)^{1/n} \frac{n}{1+n}\left(r^{\frac{n+1}{n}} - a^{\frac{n+1}{n}}\right) \tag{5.59}$$

The volumetric flowrate may be obtained by integrating the velocity profile across the pipe:

$$w_L = \int_0^a 2\pi r v_x(r) dr = \int_0^a 2\pi r \left(\frac{s}{2K}\right)^{1/n} \frac{n}{1+n}\left(r^{\frac{n+1}{n}} - a^{\frac{n+1}{n}}\right) dr \tag{5.60}$$

Integrating gives

$$w_L = \frac{n\pi}{3n+1}\left(\frac{Ksa^{3n+1}}{2}\right)^{1/n} \tag{5.61}$$

Solving for the pressure drop gives

$$\frac{\Delta P}{L} = \frac{2K}{a^{3n+1}}\left(\frac{(3n+1)w_L}{n\pi}\right)^n \tag{5.62}$$

Substituting for the pressure gradient in equation (5.59) gives

$$v_x(r) = \frac{w_L(3n+1)}{\pi a^2(n+1)}\left[1 - \left(\frac{r}{a}\right)^{\frac{n+1}{n}}\right] \tag{5.63}$$

Figure 5.24 shows equation (5.63) plotted for various values of n, the power-law index. The important consequences of these for process engineering design are as follows.

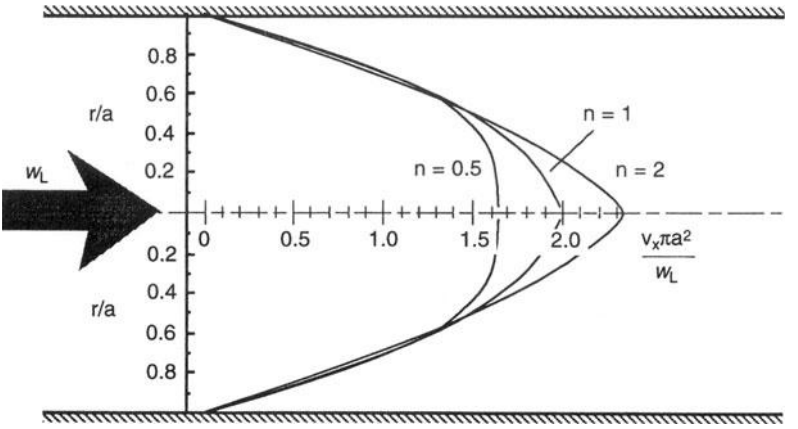

Fig. 5.24 Comparison of velocity profiles for Newtonian and non-Newtonian fluids.

- The residence time distribution of the fluid depends on the value of n. For $n < 1$ the velocity profile in Fig. 5.24 becomes flatter, resulting in more plug flow-type behaviour (see section 8.3). Similarly for $n > 1$ (shear thickening) the velocity profile becomes sharper, and a broader distribution of residence times would result.
- The pressure drop depends on the pipe radius a to the power $-(3n + 1)$, so for a Newtonian fluid $dP/dL \propto a^{-4}$ whereas for $n = \frac{1}{3}$, then $dP/dL \propto a^{-2}$, which would have important consequences for scale-up of a pipe flow.
- Heat transfer transfer coefficients may be directly correlated with the friction factor, which is related to the wall shear rate (see section 3.2, Reynolds, film and j-factor analogies). Thus shear-thinning behaviour can increase heat transfer rates, at the same throughput.

As a further example we shall investigate the behaviour of a Bingham plastic fluid in pipe flow. Following the same approach as above we can show that at a radius less than r_y, given by

$$r_y = \frac{4\tau_y}{\Delta P/L} \tag{5.64}$$

the fluid stress does not exceed the Bingham yield stress and the material moves as a central plug through the pipeline. At radii greater than r_y the fluid behaves as a Newtonian fluid and has a parabolic velocity profile, as shown in Fig. 5.25. Again, the residence time distinction and pressure drop are affected by the non-Newtonian behaviour of the fluid. Serious problems can occur with Bingham plastic fluids in more complex flow geometries: stagnant regions form where the fluid stress does not exceed the yield stress, resulting in poor rates of mixing and heat transfer.

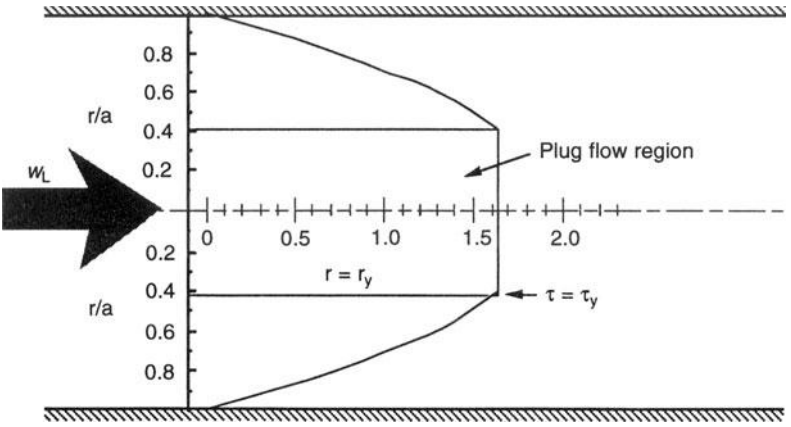

Fig. 5.25 Bingham plastic pipe flow velocity profile.

5.3.2 Complex fluid flow problems

Using the examples above it should now be obvious that laminar flow problems may be solved using similar approaches to those for a Newtonian fluid, but replacing the shear stress terms with a suitable non-Newtonian constitutive equation. The examples considered here are simple, one-dimensional problems, to which there are analytical solutions. For complex engineering geometries, the flows may be fully three-dimensional, or unsteady, and an algebraic solution to the resulting set of equations may not be possible. This is also true of many Newtonian flows; however, recent advances in computational fluid dynamics have resulted in a number of commercial software packages that are able to calculate numerical solutions to these problems. These packages solve the Navier–Stokes and continuity equations (the full three-dimensional equations of fluid motion) and are able to handle simple rheological models, such as a power-law fluid. The ability to perform calculations with viscoelastic fluids is limited, although a few (more academic) packages are available. Currently much research is being carried out on the appropriate forms of constitutive equation to model real non-linear viscoelastic materials and also to extend the current techniques of fluid mechanics to higher Reynolds number flows, even into the turbulent regime.

Appendix 5.A Linear viscoelastic Maxwell element

Referring to Fig. 5.7, the total shear stress and strain are

$$\tau = \tau_1 = \tau_2 \tag{A5.1}$$

and

$$\gamma = \gamma_1 + \gamma_2 \tag{A5.2}$$

so that

$$\dot{\gamma} = \dot{\gamma}_1 + \dot{\gamma}_2 \tag{A5.3}$$

For the Hookean spring

$$\dot{\gamma}_1 = \frac{\dot{\tau}_1}{G} \tag{A5.4}$$

and the Newtonian dashpot

$$\dot{\gamma}_2 = \frac{\tau_2}{\mu} \tag{A5.5}$$

which leads to

$$\frac{d\tau}{dt} + \frac{\tau}{\lambda} = G\dot{\gamma} \tag{A5.6}$$

where $\lambda = \mu/G$ is a relaxation time.

Solving this first-order ordinary differential equation using an integrating factor:

$$\tau(t) = G\int_{-\infty}^{t} \exp\left(-\frac{t-t'}{\lambda}\right)\dot{\gamma}(t')\,dt' \tag{A5.7}$$

Suppose now that

$$\gamma = \gamma_o \sin \omega t \tag{A5.8}$$

giving a strain rate of

$$\dot{\gamma} = \dot{\gamma}_o \omega \cos \omega t \tag{A5.9}$$

which on substitution into equation (A5.7) and integrating gives

$$\tau(t) = \frac{G\lambda^2\omega^2}{(1+\lambda^2\omega^2)}\,\gamma_o \sin \omega t + \frac{G\lambda\omega}{(1+\lambda^2\omega^2)}\,\gamma_o \cos \omega t \tag{A5.10}$$

or

$$\tau(t) = G'\gamma_o \sin \omega t + G''\gamma_o \cos \omega t \tag{A5.11}$$

Appendix 5.B Concentric cylinder viscometer

Referring to Figs 5.12 and 5.26:

$$\dot{\gamma} = \frac{(r+dr)(\omega+d\omega) - (r+dr)\,\omega}{dr} = r\frac{d\omega}{dr} \tag{A5.12}$$

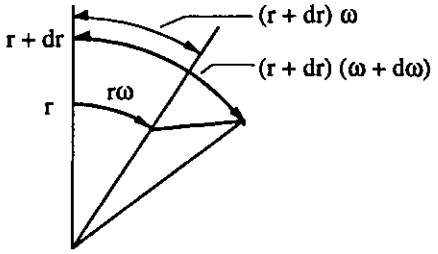

Fig. 5.26 Fluid motion in a circular path.

In steady shear

$$\Gamma_1 = -2\pi r^2 \tau L \tag{A5.13}$$

where τ is the fluid shear stress at radius r, and

$$\tau = \mu_a \dot{\gamma} \tag{A5.14}$$

If the gap is small, then $\dot{\gamma}$ and μ_a are almost constant. Then

$$\mu_a r^3 \frac{d\omega}{dr} = \frac{-\Gamma_1}{2\pi L} \tag{A5.15}$$

and integrating using the boundary conditions $\omega = \omega$ at $r = r_1$ and $\omega = 0$ at $r = r_2$ gives

$$\mu_a = \frac{\Gamma_1}{4\pi\omega L}\left[\frac{1}{r_1^2} - \frac{1}{r_2^2}\right] \tag{A5.16}$$

The shear stress varies as

$$\dot{\gamma} = \frac{\left(2\omega/r^2\right)\left(r_1^2 r_2^2\right)}{\left(r_2^2 - r_1^2\right)} \approx \frac{r_1 \omega}{r_2 - r_1} \tag{A5.17}$$

for $r_1 / r_2 > 0.96$.

Appendix 5.C Cone and plate viscometer

Referring to Fig. 5.14, in a cone and plate viscometer, the shear rate is constant, independent of radius r:

$$\dot{\gamma} = \frac{\omega r}{r \tan\theta} = \frac{\omega}{\tan\theta} \tag{A5.18}$$

The torque acting on an elemental area of $2\pi r\, dr$ is

$$d\Gamma = 2\pi r^2 \mu_a \dot{\gamma} dr = \frac{2\pi r^2 \omega \mu_a}{\tan\theta} dr \tag{A5.19}$$

Integrating from $r = 0$ to $r = R$ gives

$$\mu_a = \frac{3\Gamma \tan\theta}{2\pi R^3 \omega} \tag{A5.20}$$

Conclusions

In the introduction to fluid mechanics in Chapter 2, the discussion centred on two idealized models of a fluid: one in which it could be assumed to be frictionless and the other in which it was assumed to have Newtonian properties. A Newtonian liquid is one whose rheology is described by a single constant parameter – its viscosity.

Many food materials don't fall into either of these categories, and instead also exhibit some of the properties we usually associate with deformable or elastic solids. This chapter has dealt with ways of characterizing and classifying such non-Newtonian fluids. The quantitative models for these fluids, that is the relationships between the shear stress (or apparent viscosity) and shear rate are known as the constitutive equations. You should understand the difference between fluids whose properties are time-independent and time-dependent. Three principal categories of time-independent fluid were introduced here: shear thinning, shear thickening and Bingham plastics. The latter are fluids which behave like solids when the shear is small, but begin to flow or yield at some critical shear stress. This chapter should have given some physical insight into why these different types of behaviour exist as well as introducing some of the simpler mathematical models to describe them. Two different types of time-dependent behaviour were also introduced. Thixotropic and rheopectic fluids are examples of the first, in which changes in the physical structure lead to changes in viscosity with time. Another category of fluid exhibits both Newtonian and elastic properties, and this also results in a response to deformation which is time-dependent. These are the viscoelastic fluids. As well as meeting these different classes of fluid and real examples of food materials which approximate to them, you will have encountered some of the more common methods of measuring their properties, that is of estimating the parameters in the constitutive equations. The final part of the chapter shows how the behaviour of some of these fluids in simple pipe flow can be predicted using the methods of Chapter 2. As a result you should be able to recognize how the velocity distribution of a fluid being pumped along a pipe depends on its rheology, and how the power requirements for pumping can be predicted.

References and further reading

Barnes, H.A., Hutton, J.F. and Walters, K. (1989) *An Introduction to Rheology*

Casson, N. (1959) A flow equation for pigmented-oil suspension of the printing ink type, in *Rheology of Dispersed Systems* (ed. C.C. Mill), Pergamon Press, New York, pp. 84–104.

Cross, J.M. (1965) Rheology of non-Newtonian flows: equation for pseudoplastic systems. *Journal of Colloid Science*, **20**, 417–437.

Kreiger, I.M. and Maron, S.H. (1954) Direct determination of flow curves on non-Newtonian fluids. *Journal of Applied Physics*, **25**, 72–75.

Mackley, M.R. (1988) in *The Physical Principles of Rheological Measurement* (eds A.A. Colyer and D.W. Clegg), Elsevier, Chapter 1.

Nielsen, L.E. (1977) *Polymer Rheology*, Marcel Dekker.

Prentice, J.H. and Huber, A.N. (1983) Measuring rheological properties of foodstuffs, in *Physical Properties of Foods* (eds R. Jowitt, F. Escher, B. Hallstrom, H.F.Th. Meffert, W.E.L. Spies and G. Vos), Applied Science Publishers, pp. 123–184.

Reynolds, O. (1885) *Philosophical Magazine*, [5] **20**, 469.

Steffe, J.F. (1992) *Rheological Methods in Food Process Engineering*, Freeman Press, Michigan.

Steventon, A.J., Parkinson, C.J., Fryer, P.J. and Bottomley, R.C. (1991) The rheology of yoghurt, in *Rheology of Food, Pharmaceutical and Biological Materials with General Rheology* (ed. R.E. Carter), Elsevier Applied Science, pp. 196–210.

Tanner, R.I. (1985) *Engineering Rheology*, Clarendon Press, Oxford.

Tiu, C. and Boger, D.V. (1974) Complete rheological characterization of time-dependent products. *Journal of Texture Studies*, **5**, 329–338.

Tritton, D.J. (1988) *Physical Fluid Dynamics*, 2nd edn, Chapman & Hall, London.

Walters, K. (1975) *Rheometry*, Chapman & Hall, London.